Real-Time PMD Tolerance Measurements of a PIC-Based 500 Gb/s Coherent Optical Modem

Jeffrey T. Rahn, *Senior Member, IEEE*, Han Sun, *Member, IEEE*, Kuang-Tsan Wu, *Senior Member, IEEE*, and Bert E. Basch, *Senior Member, IEEE, Member, OSA*

***Abstract*—We present real-time polarization mode dispersion (PMD) tolerance measurement results with a commercially available 500 Gb/s coherent modem. The first- and second-order PMD space is explored, showing that peak values of 500 ps of static, first-order PMD (differential group delay) have small penalties. The system was stressed using fast scrambling, with polarization change of over 10 000 rad/s, along with high mean PMD. Penalties were small with sufficient equalization.**

***Index Terms*—Integrated optics, optical fiber communication, optical fiber dispersion, phase modulation.**

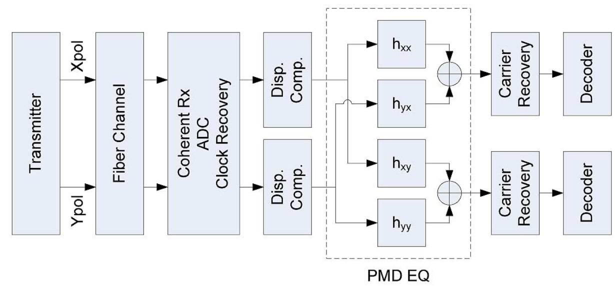

Fig. 1. Modern coherent optical system architecture.

I. Introduction

NEAR perfect compensation of polarization mode dispersion (PMD) is one of the important features for a coherent receiver (RX). In this paper, we report the real-time PMD tolerance measurement results of a photonic integrated circuit (PIC)-based 500 Gb/s coherent modem. Two conditions were analyzed: first, PMD was stepped to specific PMD values and the bit error ratio (BER) performance for each PMD value was determined. This experiment shows the dependence on the number of active equalization taps. Second, transient PMD was generated using fixed differential group delay (DGD) elements separated by polarization rotators, with the rotators inducing polarization slew rates over 10 000 rad/s. This test shows robustness to time varying polarization and PMD. We believe that the PMD tolerance results presented here constitute the highest reported for real-time, digital coherent RXs.

PMD experienced on installed fiber typically results from random variations in birefringence in distributed, short sections of fiber, each of which introduces DGD. As the state of polarization between fiber segments changes, the total amount of PMD varies. For this paper, the PMD for a static fiber configuration can be characterized by the first-order and second-order PMD values, where the static first-order PMD is the DGD. A dynamic link is characterized by its mean DGD value. The instantaneous first-order PMD values in a dynamic link follow a Maxwellian distribution, so 99.999% of the occurrences of first-order PMD are below 3.18 times the mean PMD value (mean DGD).

Manuscript received March 22, 2012; revised May 14, 2012, May 31, 2012; accepted June 29, 2012. Date of publication July 10, 2012; date of current version August 24, 2012.

J. T. Rahn is with Infinera Corporation, Sunnyvale, CA 94087 USA (e-mail: jrahn@infinera.com).

H. Sun and K.-T Wu are with Infinera Canada, Inc., Ottawa, ON K2K 2X3, Canada (e-mail: hsun@infinera.com; kwu@infinera.com).

B. E. Basch is with Verizon Laboratories, Waltham, MA 02451 USA (e-mail: bert.e.basch@verizon.com).

Color versions of one or more of the figures in this paper are available online at http://ieeexplore.ieee.org.

Digital Object Identifier 10.1109/JLT.2012.2207946

II. PMD Compensation Using Linear Equalization

A modern coherent optical system can be represented as in Fig. 1. A polarization-multiplexed (PM) quadrature phase shift keying (QPSK) signal is generated, propagated through fiber, and detected using coherent techniques [1], [2]. After clock recovery and dispersion compensation, the two complex signals enter the equalizer block indicated as "PMD EQ," which is the main focus of the present discussion. Coherent modulation formats such as PM-QPSK are a linear modulation and PMD experienced in the fiber is a linear distortion. As such, it is effective to use a linear equalizer to compensate PMD. The PMD equalizer has two inputs and two outputs and consists of four sets of complex tap weights, h_{xx}, h_{yx}, h_{xy}, and h_{yy}. Fig. 2 illustrates the time-domain structure for h_{xx}, which is an N-tap transversal equalizer (with D being the tap delay), which can also be implemented in the frequency domain [3] for more efficient computation when the number of taps is large. For effective PMD compensation, D should be less than baud interval (T, also called one unit interval: UI). For example, $D = T/2$ is commonly used, but it is possible to use D greater than $T/2$ [4].

The equalizer span $(N-1) \times D$ (or $(N-1) \times D/T$ UI), the delay between the first and last taps, must be larger than the DGD introduced in the fiber, in addition to any requirement for compensating intersymbol interference (ISI) and/or tracking clock wander. When designed properly, the performance of the PMD equalizer depends upon the equalizer span and is the same regardless of time- or frequency-domain implementation. As such, we report the performance of PMD equalizer versus the equalizer span measured in the unit of UI. The tap-weight updating algorithms, least-mean square and constant modulus algorithm [5], are implemented. In order for the PMD equalizer

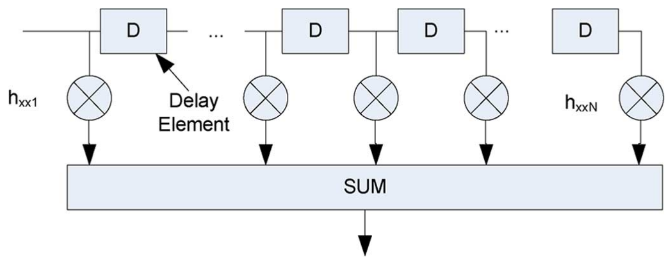

Fig. 2. Linear transversal equalizer structure. For *T*/2 spaced taps, the delay *D* would be set to half of the baud period, *T*/2.

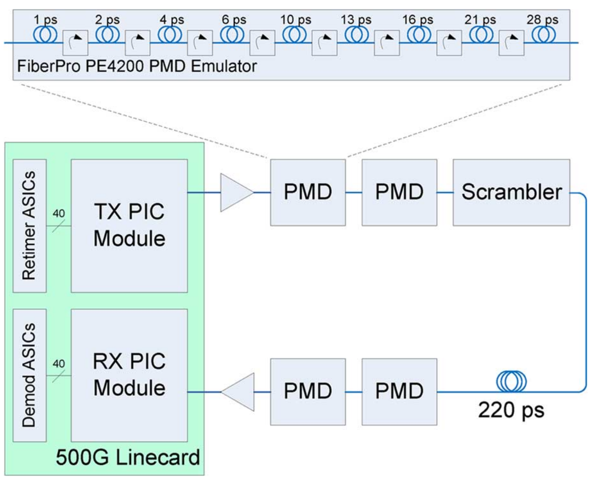

Fig. 3. Measurement setup.

to perform well, the coherent RX requires robust clock recovery which tolerates half UI DGD [6], [7].

III. Measurement Setup

A production 500G modem was used to generate and receive the signals for this experiment [8]. The test setup is shown in Fig. 3. The transmitter (TX) uses the PRBS15 generator in the retimer application-specified integrated circuit (ASIC). Forty high-speed signals arrive at the TX module where they are amplified by the SiGe driver ASIC to drive the Mach–Zehnder modulators on the InP PIC. These signals modulate the integrated distributed feedback (DFB) lasers to produce 10 14.25 GBaud (57 Gb/s) PM-QPSK signals on a 200 GHz grid, which are wavelength multiplexed prior to exiting the PIC.

A high-gain erbium-doped fiber amplifier provides optical noise loading to achieve an output BER better than the typical capability of hard forward error correction (FEC) implementations (Actual BER range was 4E-4 to 1.7E-3 due to small variation of signal-to-noise ratio across the channels.). The optical signal returned after noise loading is shown in Fig. 4.

The signal returns to the RX PIC module where the wavelengths are demultiplexed, combined with a per channel local DFB laser using a pair of 90° hybrids, one for each polarization, and delivered to balanced photodiode pairs. The 40 high-speed signals are amplified within the module using a SiGe ASIC, then delivered to 5 digital signal processing ASICs (fabricated in 40 nm CMOS), with each ASIC processing two wavelengths. Signal processing within that ASIC removes the impact of PMD, polarization rotation, offset between the TX and RX

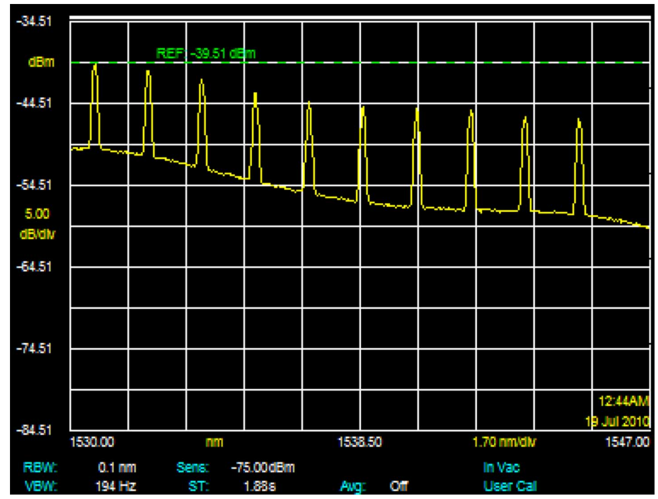

Fig. 4. Optical spectrum at RX in experimental configuration.

lasers' phase and frequency, and offset from the TX and RX clocks. Fig. 5 shows a photo of the test set.

PM formats have degenerate solutions at the receive equalizer due to the possibility of shifting the X- and Y-polarization signals by integer UI when CMA algorithm is used. A system implementation might resolve this degeneracy by observing X- and Y-polarization frame-alignment words (e.g., as in FEC framing), and resetting the equalizer tap coefficients once integer UI skews are found. Since this experiment was conducted using unframed pseudorandom binary sequences (PRBS), the equalizer initialization was performed with low-channel PMD values, and the equalizer was verified to be in the optimal configuration.

The error rate is determined from the recovered data, using the PRBS checkers within the demodulation ASIC. These error counters run continuously and count all errors within the gating time. The counter logic declares an out-of-lock condition if the error rate exceeds a threshold in order to catch high ($>$10%) error-rate bursts. This condition was not present for data presented in this paper. In the following discussion, the Q value is inferred from the BER as $\mathrm{BER} = 1/2 \ \mathrm{erfc}\ (Q_{\mathrm{LIN}}/\sqrt{2})$, $Q_{\mathrm{dB}} = 20 \log_{10} Q_{\mathrm{LIN}}$, and all Q penalties are referenced to the Q values without PMD. Q values are determined independently for each wavelength.

IV. Static PMD

For this experiment, four PMD emulators (FiberPro PE4200) were configured to maintain a fixed 100 ps DGD; the first rotator in each PE4200 was set randomly in order to generate a distribution of first- and second-order PMD. Once each was set, the equalizer taps and BER values were determined. In this configuration, the scrambler shown in Fig. 3 was disabled.

The tap values were analyzed to determine the PMD compensated by the equalizer. The equalizer taps, when optimally adapted, should invert the Jones matrix of the optical link. The tap coefficients can therefore be analyzed to give a reliable estimate of the polarization modification between the TX and RX. Assigning the equalizer tap weights in frequency domain to be equivalent to the 2×2 complex transmission matrix $T(\omega)$

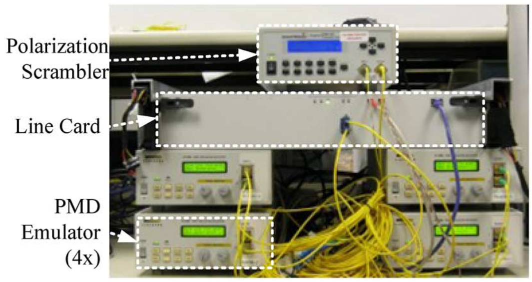

Fig. 5. Measurement setup. The polarization scrambler is at the top, the line card in the middle, and four PMD emulators at the bottom.

which is a function of ω, the frequency offset from the transmit laser. The unitary matrix $U(\omega)$ can be computed as follows [9]:

$$H(\omega) = [T(\omega)T(\omega)^{\dagger}]^{\frac{1}{2}}$$
$$U(\omega) = H(\omega)^{-1}T(\omega).$$

The principal states of polarization can then be obtained by computing the eigenvectors of M

$$M = j\left.\frac{dU(\omega)}{d\omega}\right|_{\omega=0} U(0)^{-1}$$

with the first-order PMD value obtained as the corresponding eigenvalues of M.

The second-order PMD consists of the parallel component, the derivative of the first-order PMD with respect to frequency, and the perpendicular component, the derivative of the principle states of polarization with respect to frequency. The root-mean square of these two values represents the total second-order PMD.

In order to validate this technique for determining first- and second-order PMD, a polarization emulator was connected to generate the appropriate PMD. The values generated by the emulator were compared with the values reported by the tap computation discussed previously. These are shown in Fig. 6, with the error bars representing the 1-σ variation in the reported value.

The experiment progressed as follows. First, the rotators within the PMD emulators were randomly set to induce a PMD condition on the link. Next, with the rotators fixed, the Q value was measured, and the taps were extracted from the DSP ASIC to determine PMD. This was repeated to get a dense collection of PMD values, Q values, and wavelength. First- and second-order PMD values were placed into bins, 30 ps $\times$ 200 ps^2 wide, and BER values whose PMD values fell within the bin were averaged. Wavelength dependence was small (Q penalty values had $\sigma = 0.02$ dB between wavelengths), so penalties shown below are averaged across wavelength after binning by PMD value.

In the first experiment using the four emulators and an equalizer span of 8 UI, a PMD tolerance of 330 ps of static first-order PMD (DGD) or 35 000 ps^2 of static second-order PMD was demonstrated with less than 0.1 dB penalty. The Q penalty, based on 28 000 $\mathrm{PMD} + Q$ measurements, is shown in Fig. 7.

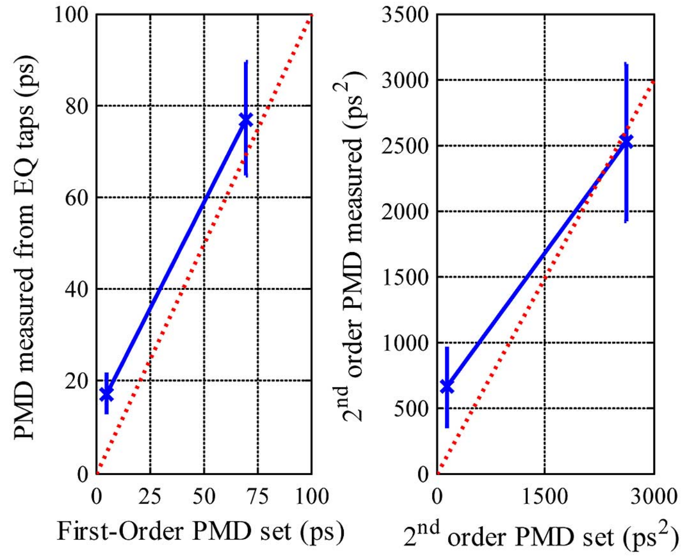

Fig. 6. Comparison of setpoints on FiberPro PMD emulator with readout from equalizer taps.

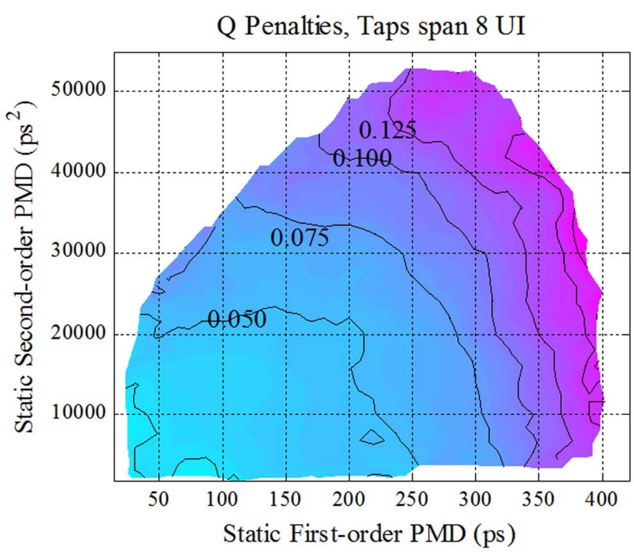

Fig. 7. Q penalty (contours shown with labels in dB) versus PMD for eight UI tap span.

In a second experiment, the spool of PM fiber with 220 ps of DGD was included, and the equalizer time span was extended to 12 UI. This configuration tolerates 550 ps of static first-order PMD (DGD) or 70 000 ps^2 of static second-order PMD. The Q penalty, based on 17 000 $\mathrm{PMD} + Q$ measurements, is shown in Fig. 8.

V. PMD Transients Test

A crucial property of coherent RXs is the capability to compensate for time-varying PMD. Polarization transients can be induced by mechanical vibration and maintenance activities, and

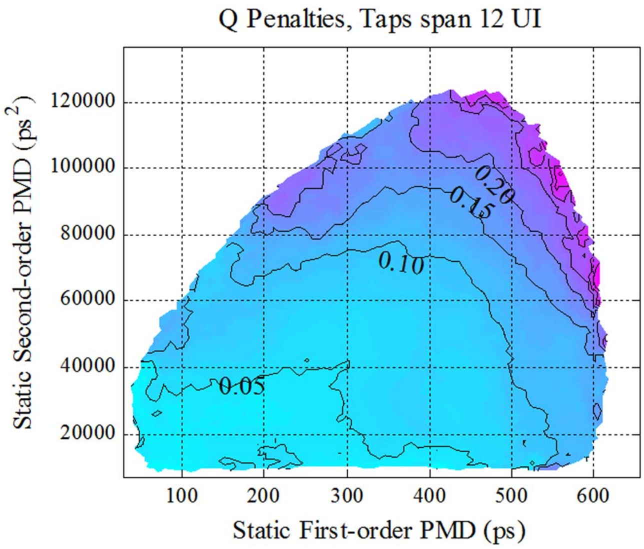

Fig. 8. Q Penalty (in dB) versus static PMD for 12 UI tap span.

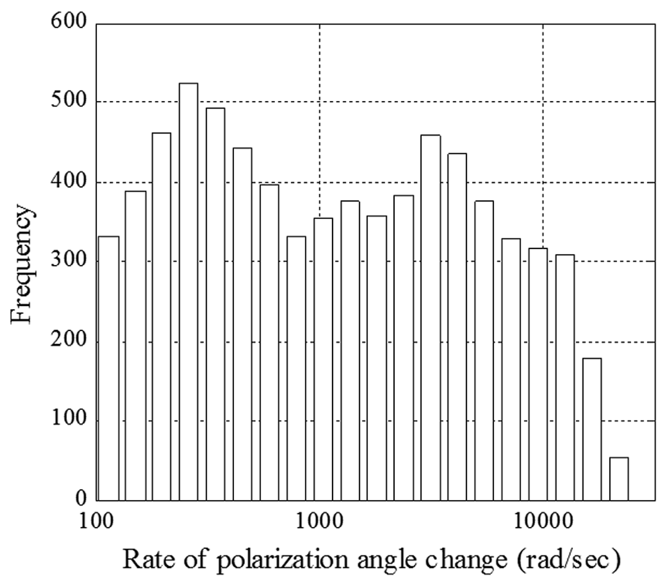

Fig. 9. Distribution of rate of change of polarization with PSY-101.

systems need tolerance within the acoustic range. A demonstration of PMD tolerance would be incomplete without including rapid polarization transients.

The polarization rotation rate for the General Photonics polarization controller (labeled "Scrambler" in Fig. 3) was measured in order to benchmark the polarization tracking experiment, when set to its fastest rate (labeled "6000 Hz"). Repeated measurements of the state of polarization were taking with a fast polarization analyzer, and the slew rate was measured repeatedly. The distribution of rate of polarization angle change is shown in Fig. 9. Peak transient rates exceed 10 krad/s. All measurements in this section were taken with scrambler operating at its fastest rate.

The DSP allows the number of active taps in the equalization stage to be adjusted. This enables a study of the impact of the time span of the equalization versus the PMD penalty. Without

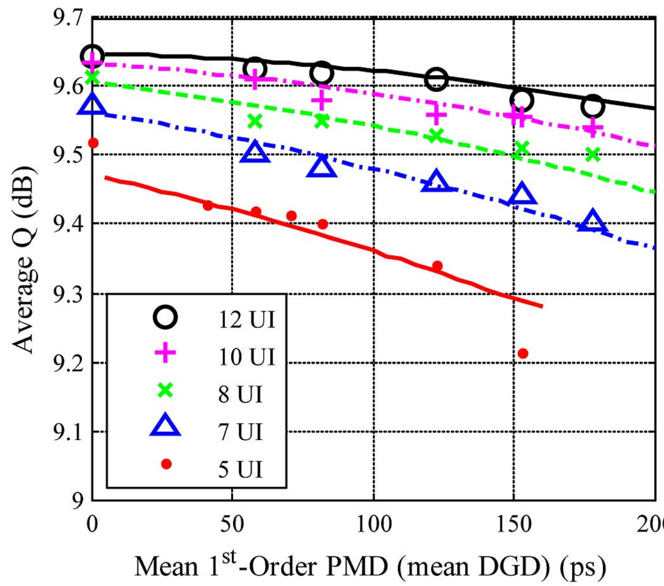

Fig. 10. Performance of coherent equalizer with varying numbers of active taps, under the stress of dynamic PMD.

added PMD, there is a small benefit to increasing the number of active taps. This results from compensation of ISI, where the ISI comes from the TX, RX, and optical bandwidth restrictions. The simplest approximation for the impact of additional PMD on the system performance is to model the added PMD compensation as further eroding the ISI compensation ability of the equalizer. A simple model was used to determine the penalty Q_T as a function of the number of active taps

$$Q_T(N_T) = Q_0 - \alpha(N_T - N_0)^2.$$

Parameters are obtained using a least-squares fit to the data, obtaining $\alpha = 0.00315$ and $N_0 = 12$ UI. Since the measurement is performed using statistical PMD emulation, the mean Q value is evaluated by convolving the Q penalty with the probability of observing a given PMD delay τ, assuming a Maxwellian distribution $P(\tau)$

$$\langle Q \rangle = \int_0^\infty Q_T\left(N_T - \frac{\tau}{T}\right) P(\tau) d\tau.$$

Fig. 10 includes this modeled PMD penalty, along with average Q values. Channel dependence was small (Q penalties had $\sigma = 0.036$ dB across channels) and was averaged for each DGD and tap configuration. Note that the peak penalties are higher as the polarization scrambling is rapid compared with the BER integration time. Also note that the mean values of PMD with a random distribution will have different average Q values than the static performance shown in Fig. 8.

The modem was operated with the scrambling enabled, while 22 000 sets of tap values of the PMD equalizer were collected. As shown in Figs. 11 and 12, up to 250 ps/15000 ps^2 of first/second-order PMD was observed. Note the good agreement with expected Maxwellian distribution [10], [11] for

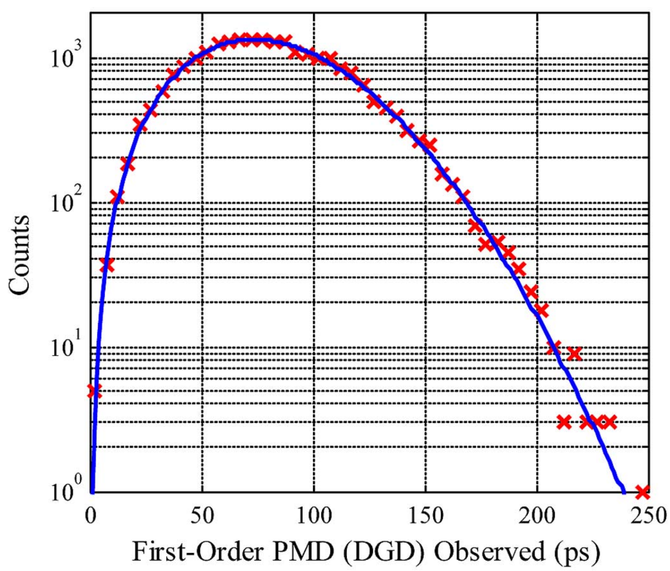

Fig. 11. Measured histogram of first-order PMD. Solid line indicates curve fit assuming Maxwellian distribution.

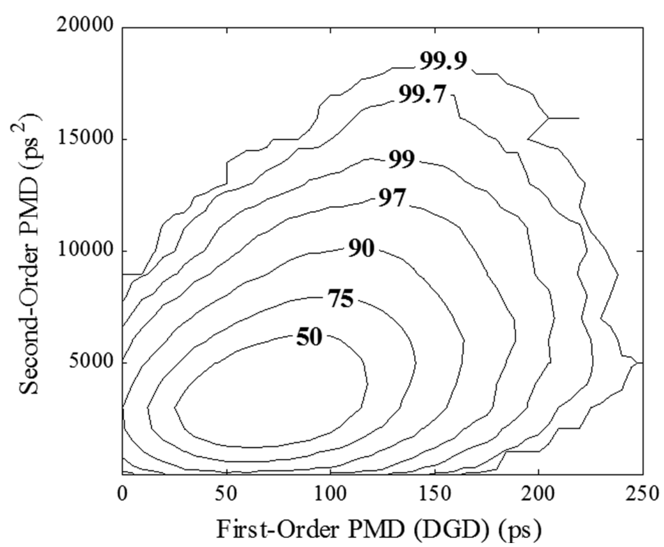

Fig. 12. Measured distribution of first- and second-order PMD. Labels indicate percentage of the distribution contained within that contour.

first-order PMD, shown in the solid line on the plot of Fig. 11. The contour plot of Fig. 12 shows the likelihood of landing on a given location in the first- and second-order PMD space. Given the rapid scrambling rates, the space within the 99% contour should be covered at a fine resolution every few seconds. The half-UI DGD setting, which can be particularly problematic for clock recovery, will be passed through dozens of times each second.

The BER values were collected using 1-s integration time, which is slow compared to the polarization rotation rate. There are two objectives to this experiment: first, to demonstrate that all controls (equalizer and clock recovery) are stable in the presence of the DGD and transient combinations; second, to demonstrate that BER values are stable. Q values for all wavelengths taken over a 10 h time span are shown in Fig. 13. Q values are observed to vary by less than 0.18 dB, indicating no loss-of-lock

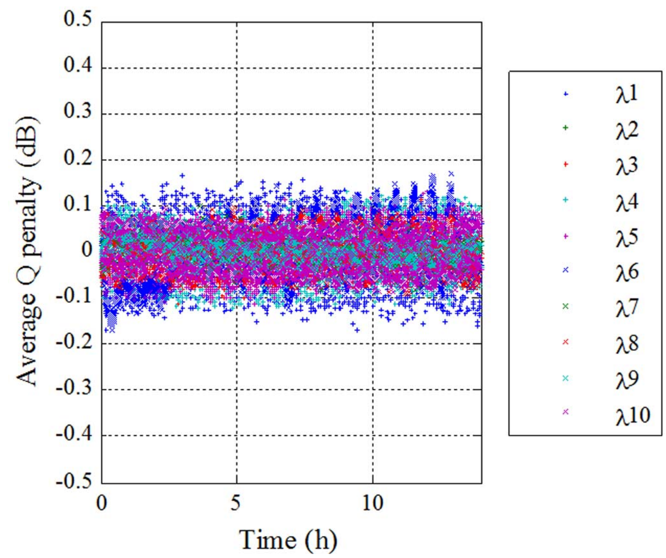

Fig. 13. Q variation versus time under stressed PMD conditions.

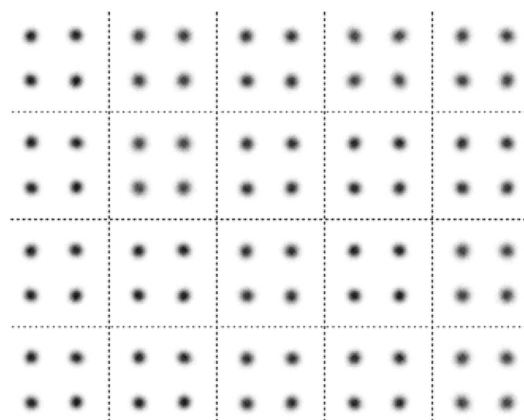

Fig. 14. Constellation diagrams recorded during stressed PMD experiment.

events, stable BER values during this soak experiment, and no rare PMD conditions causing out-of-family BER.

Constellation diagrams for all ten wavelengths were also collected in order to show the signal quality at the equalizer output, shown in Fig. 14.

VI. Conclusion

We have demonstrated a coherent optical modem which can handle large PMD values. The first- and second-order PMD space is explored, showing that peak values of 500 ps of static, first-order PMD (DGD) have small penalties. The coherent RX is also tolerant of rapid polarization transients.

Acknowledgment

The authors would like to thank Infinera engineering community for building the 500 GB/s PICs and linecard used in these experiments.

References

[1] M. G. Taylor, "Coherent detection method using DSP for demodulation of signal and subsequent equalization of propagation impairments," *IEEE Photon. Technol. Lett.*, vol. 16, no. 2, pp. 674–676, Feb. 2004.

[2] M. Kuschnerov, F. N. Hauske, K. Piyawanno, B. Spinnler, M. S. Alfiad, A. Napoli, and B. Lankl, "DSP for coherent single-carrier receivers," *J. Lightw. Technol.*, vol. 27, no. 16, pp. 3614–3622, Aug. 15, 2009.

[3] J. J. Shynk, "Frequency-domain and multirate adaptive filtering," *IEEE Signal Process. Mag.*, vol. 9, no. 1, pp. 14–37, Jan. 1992.

[4] C. Malouin, B. Zhang, A. Wagner, S. Khatana, E. Ibragimov, H. Jiang, and T. Schmidt, "Sub-rate sampling in 100 Gb/s coherent optical receivers," in *Proc. Opt. Fiber Commun. Conf.*, 2010, pp. 1–3.

[5] D. N. Godard, "Self-recovering equalization and carrier tracking in two-dimensional data communication systems," *IEEE Trans. Commun.*, vol. COM-28, no. 11, pp. 1867–1875, Nov. 1980.

[6] H. Sun and K.-T Wu, "A novel dispersion and PMD tolerant clock phase detector for coherent transmission systems," in *Proc. Opt. Fiber Commun. Conf.*, 2011, pp. 1–3.

[7] F. N. Hauske, "Impact of optical channel distortions to digital timing recovery in digital coherent transmission systems," in *Proc. Int. Conf. Transp. Opt. Netw.*, 2010, pp. 1–4.

[8] F. Kish, R. Nagarajan, M. Kato, P. Evans, S. Corzine, M. Ziari, A. Nilsson, J. Rahn, D. Lambert, A. Dentai, V. Lal, M. Fisher, M. Kuntz, A. James, R. Malendevich, G. Goldfarb, H.-S. Tsai, P. Samra, H. Sun, J. Stewart, T. Butrie, J. McNicol, K.-T. Wu, M. Reffle, and D. Welch, "Coherent large-scale InP photonic integrated circuits," in *Proc. 37th Eur. Conf. Opt. Commun.*, 2011, pp. 1–3.

[9] C. D. Poole and R. E. Wagner, "Phenomenological approach to polarisation dispersion in long single-mode fibres," *Electron. Lett.*, vol. 22, no. 19, pp. 1029–1030, Sep. 11, 1986.

[10] G. J. Foschini, L. E. Nelson, R. M. Jopson, and H. Kogelnik, "Probability densities of second-order polarization mode dispersion including polarization dependent chromatic fiber dispersion," *IEEE Photon. Technol. Lett.*, vol. 12, no. 3, pp. 293–295, Mar. 2000.

[11] G. J. Foschini, L. E. Nelson, R. M. Jopson, and H. Kogelnik, "Statistics of second-order PMD depolarization," *J. Lightw. Technol.*, vol. 19, no. 12, pp. 1882–1886, Dec. 2001.

Jeffrey T. Rahn (S'93–M'92–M'98–SM'12) received the B.Sc. degree in physics from Stanford University, Palo Alto, CA, in 1991, and the Ph.D. degree from the University of California at Santa Cruz, Santa Cruz, in 1998. His thesis experimental work was performed at Deutsche Electronen Synchrotron, Hamburg, Germany, on deep inelastic scattering of electrons and protons.

From 1998 to 1999, he held a postdoctoral position with Xerox's Palo Alto Research Center, Palo Alto, and then joined Acuson Corporation, developing signal processing algorithms for medical ultrasound. In 2001, he joined Big Bear Networks, where he was involved in the development of electronic dispersion compensation application-specified integrated circuits for 10 GB/s receivers running over single-mode and multimode fibers. He played a key role in the successful introduction of technology used in 10 GBase-LRM. In 2005, Big Bear was acquired by Infinera Corporation, Sunnyvale, CA, where he has been involved in optical architecture for their long-haul networking gear and has continued his role in signal processing. On the optical signal processing front, he has developed and integrated the planar lightwave circuits, including demonstrating a novel technique for performing phase modulation differential quadrature phase shift keying demodulation using a combination of optical, analog electrical, and digital signal processing. He has been recently involved in architecture and integration of coherent optical systems. He holds seven patents.

Han Sun (M'12) received the B.Eng. degree in electrical engineering and M.A.Sc. degree in photonics and semiconductor lasers from the University of Toronto, Toronto, ON, Canada, in 1997 and 1999, respectively.

From 2001 to 2009, he was with Nortel, Ottawa, ON, where he was involved in research on future optical transport systems. From 2003 to 2006, he was instrumental in the development of DSP algorithms which led to the World's first commercial 40 Gb optical modem employing Pol-Mux quadrature phase shift keying modulation format. He is currently with Infinera Canada, Ottawa, architecting the next-generation transceivers targeting at 100 Gb and beyond. He holds 16 granted U.S. patents and 23 additional submissions. He has authored or coauthored more than 22 technical journals papers and conference presentations. His research interests include signal processing, receiver equalization, and error correction coding.

Kuang-Tsan Wu (M'81–SM'12) received the B.S. and M.A.Sc. degrees from National Taiwan University (NTU), Taipei, Taiwan, in 1975 and 1979, respectively, and the Ph.D. degree from the University of Ottawa, Ottawa, ON, Canada, in 1986, all in electrical engineering.

He was an Instructor at the National Taiwan Institute of Technology and NTU from 1979 to 1982. He was involved in research on satellite modems at Microtel Pacific Research, Burnaby, BC, Canada, during 1986–1987. He moved back to Ottawa in 1987 to join BNR and was the key System Designer for the world's first 512-quadrature amplitude modulation digital radio. From 1994 to 1995, he was with wireless R&D Group, CCL/ITRI, Taiwan, developing a digital-enhanced cordless telecommunication system. At Nortel, he was involved in research on GSM and fixed broadband wireless system, where he later joined the Metro Ethernet Networks Division in 1999 and led the system design of the 40G coherent optical modem in which the receiver application-specified integrated circuit worked without any respin. Since May 2009, he has been with Infinera Canada, Ottawa, where he leads the Ottawa Design Center. He is applying coherent technologies in conjunction with photonic integrated circuits for current and future optical transport systems. He has been granted 25 U.S. patents and one Canadian patent. He is an Infinera Fellow.

Bert E. Basch (S'67–M'67–SM'86) received the Elektrotechnisch Ingenieur degree from the Delft University of Technology, Delft, The Netherlands, in 1967.

In 1969, he joined GTE Laboratories, where he was involved in research on a wide variety of projects, mostly in the development of advanced communication systems and networks. He was responsible for GTE's pioneering research in optical communication systems, which led to the deployment of the world's first fiber optic communication system in the public switched telephone network, the first transport of broadcast TV over fiber in the U.S., and the installation of a 140 Mb/s system in Belgium that at the time of installation was the highest optical transport rate to be put in service. He also conducted seminal studies on multigigabit transmission systems and coherent optical communications. He developed the technical requirements for GTE's fiber to the home trial in Cerritos and directed all of GTE's major fiber optic field trials. In 2000, after GTE's merger with Bell Atlantic, he joined Verizon Network and Technology, Waltham, MA. His evaluation of network architectures resulted in the adoption of a reconfigurable optical add–drop multiplexer (ROADM) infrastructure, and integration of switching functionality in the transport platform. He also developed the key optical specifications for the design of Verizon's long-haul network infrastructure, and initiated the testing of 100 Gb/s and beyond transmission systems in Verizon's network. More recently, he developed the optical specifications, including the use of flexible grid ROADM technology and elastic optical networking, for a new nationwide network that Verizon has started to build. He is the author or coauthor of numerous research papers, as well as review articles, and several book chapters. He is also the Editor of the book *Optical Fiber Transmission* (Indianapolis, IN: Sams Publishing, 1987), with the introduction chapter cowritten with C. Kao. He holds 13 patents.

Mr. Basch was the Guest Editor for the IEEE/JOURNAL OF LIGHTWAVE TECHNOLOGY special issue on Optical Fiber Communications Conference/National Fiber Optic Engineers Conference (OFC/NFOEC) 2009, 2010, and 2011. He is also the recipient of two Warner Technical Achievement Awards, GTE's highest Technical Award, for exceptional contributions to optical communication technology in 1980 and gigabit networking in 1984. He is a member of the Optical Society of America and Sigma Xi, was the General Co-Chair for OFC/NFOEC 2010, and is currently a member of the OFC/NFOEC Steering Committee.